The role of zinc in magnetic and other physical water treatment methods for the prevention of scale

PP Coetzee*, M Yacoby and S Howell

Department of Chemistry and Biochemistry, Rand Afrikaans University, PO Box 524, Johannesburg 2006, South Africa

Abstract

Zinc species released from the surface of physical water treatment devices into the feed water are shown to be primarily responsible for scale inhibition effects observed in three different types of physical water treatment (PWT) devices. The three types of PWT devices included units based on a magnetic field provided by a permanent magnet; a high frequency electric field; and a "catalytic conversion" process. Freshly released zinc from PWT devices was shown to have a marked effect on the induction period for $CaCO_3$ precipitation and on the crystal morphology of $CaCO_3$. No measurable effect on the crystallisation reaction for calcium carbonate ascribable to the magnetic or electrical fields caused by the devices under investigation could be found.

Introduction

Physical water treatment (PWT) for the prevention of scale has been actively promoted as an alternative for the chemical treatment of water since the first PWT patent was registered in 1945 (*Vermeiren, 1958*). This patent was for magnetic water treatment. Other PWT techniques include methods based on electric or electrostatic fields, "catalytic conversion" and ultrasonic vibration. Despite numerous laboratory and field studies (Busch et al., 1986; Caplan and Stegmayer, 1987; Eliassen and Uhlig, 1952; Ellingsen and Fjedsend, 1982; Kochmarsky et al., 1982; *Pandolfo et al., 1987*) to prove the effectiveness of these methods, no conclusive evidence can be presented to date. Many theories have been proposed but none is able to provide a satisfactory foundation for a mechanistic explanation of the claimed effects.

It is claimed in reviews (Baker and Judd, 1996; Van der Hoven et al., 1991) that PWT leads to:

- a decreased rate of scale formation on heat exchanger surfaces
- the formation of a soft scale with a different morphology and crystal structure characterised by weaker adhesive properties
- descaling i.e. dissolution of existing scale
- increased wetting capacity
- lowering of surface tension and viscosity of water and changes in the infrared spectrum of water
- degassing of solutions
- increased capacity of ion exchangers
- increased efficiency of flotation
- a memory effect which can last up to 72 h
- the formation of smaller crystallisation particles
- increases in solubility of slightly soluble compounds
- a decrease in zeta potentials
- inhibition of bacterial and algal growth
- an increase in crop yields
- intensification of coagulation processes
- reduction in corrosion
- various other related effects.

* To whom all correspondence should be addressed.
☎(011) 489-2363; fax (011) 489-2363; e-mail ppc@rau3.rau.ac.za
Received 19 February 1996; accepted in revised form 24 May 1996.

It was our objective to find a common denominator which would link the above-mentioned diverse effects and would make possible a plausible mechanistic explanation. We assumed that scale formation proceeds through the processes of nucleation and crystal growth on exposed surfaces or in the bulk of the liquid phase followed by the attachment of crystalline particles to a surface, forming a layer prone to further growth. If PWT was to affect scale formation at all, the effect would therefore be expected to result from a modification of the crystallisation behaviour. This might be achieved by influencing nucleation and crystal growth processes directly or indirectly by changing the physico-chemical properties of the system. The latter option was included as a possibility because of claims that changes in surface tension, viscosity, and the infrared spectrum of water were observed.

Since the $CaCO_3$ precipitation reaction is known to be extremely sensitive to impurity ions, even at ultra-trace concentration levels, the possible release of metal ions from the surface of the PWT devices and its consequences were also investigated. This idea resulted in a breakthrough in which it was established that Zn^{2+} ions released from the device surface, were actually responsible for the observed effects of crystal morphology changes and reduced nucleation rates. These effects could translate into reduced scale formation.

Three functional types of PWT device were investigated: magnetic, high frequency electric field and catalytic conversion.

Experimental

Physical water treatment devices

Type: Permanent magnet

The Polar Model PD15 illustrated in Fig. 1 was obtained from Polar International, Sandefjord, Norway. It consisted of a steel cup which housed a well-type magnet. The size of the magnetic gaps on two sides was only 1.5 mm across which enabled concentration of the magnetic field in the active region to a value of 0.7 tesla.The unit was also provided with a stainless steel strainer fitted with a central rod which acted as a collector for magnetic particles that might be present in the water to be treated. This prevented the accumulation of magnetic particles in the magnet and clogging of the magnetic gaps. A 15 mm zinc sleeve

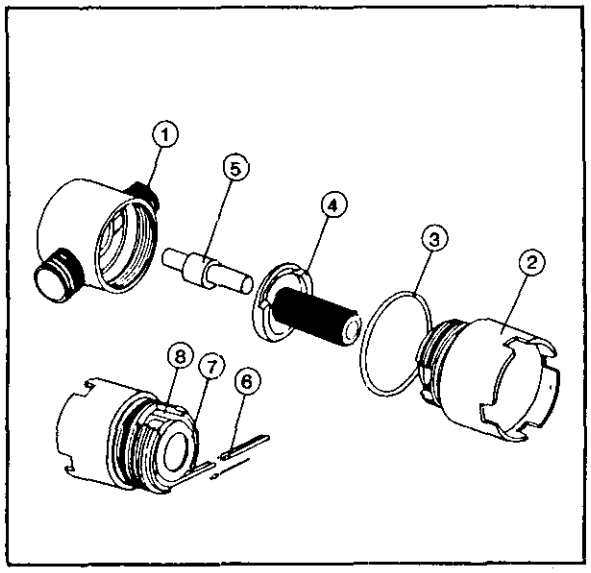

Figure 1
Diagram of Polar Model PD15 magnetic water treatment device
1) base cup
2) treatment unit
3) O-ring seal
4) strainer basket
5) magnetic rod with zinc anode
6) plastic strips for flow-rate control
7) steel pole shoe ring
8) ring shaped magnet

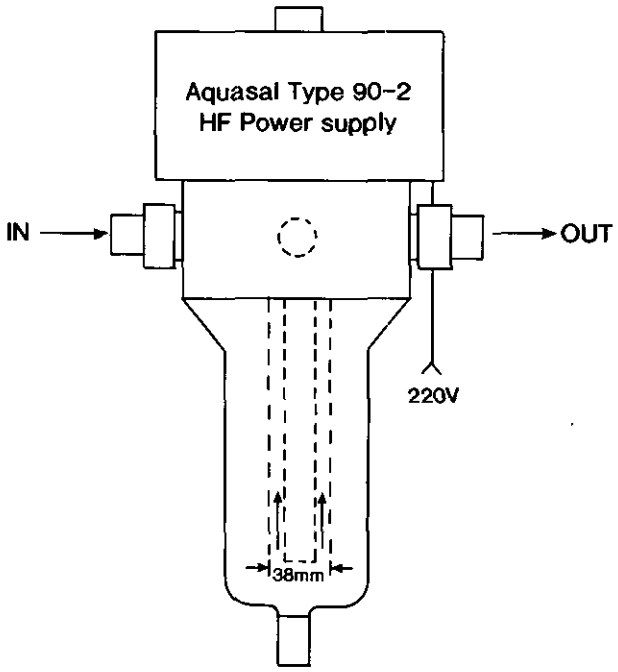

Figure 2
Diagram of Aquasal high frequency electric field water treatment device

was fitted to the rod for corrosion protection. The composition of the special alloy used in the magnet material was not disclosed by the manufacturer. The unit was specified to operate at a minimum linear flow rate of 2 $m \cdot s^{-1}$.

Type: High frequency electric field

The Aquasal Type 90-2 illustrated in Fig. 2 was obtained from Arndt Weber & Associates, Johannesburg, South Africa. It consisted of a 38 mm dia. stainless steel tube outer electrode and a 10 mm dia. stainless steel rod inner electrode mounted in a concentric fashion. The high frequency field (ca. 6000 Hz) across the electrodes consisted of square wave pulses, 14 volt positive and 18 volt negative. The relative values of the positive and negative signals changed slightly with the conductivity of the feed water. Currents increased with conductivity and values of up to 1 amp were measured at conductivities of 1 000 $\mu S.cm^{-1}$. No minimum flow rates were specified for this unit.

Type: Catalytic conversion

The PTH Model PTH 20A was obtained from PTH, Haifa, Israel. It consisted of an alloy grid made out of an unspecified selection of base and noble metals mounted in a stainless steel tube. The manufacturer specifies that the unit must be earthed when in use. Minimum flow rates of 10 *ℓ*/min were required.

Test loops

The test loops made out of 20 mm PVC piping and used for testing the devices, are depicted in Fig. 3(a) for the Polar and Fig. 3(b) for the Aquasal and PTH units. In the case of the Polar device, an exact replica made out of PVC was used for control runs. In the case of the Aquasal and PTH units, a piece of PVC tubing was inserted in place of the device when control runs were performed. Different test loops were used to allow for the substantially different minimum flow rates required by the three devices. This resulted from the fact that the Polar device was designed for household application whereas the other two were categorised as light industrial devices.

- The flow rate for the Aquasal unit was 6 *ℓ*/min. For a typical 3 *ℓ* sample the exposure rate was two times per minute in a 2.5 m circuit.
- The flow rate in the 4 m long test loop for the Polar device was 2 *ℓ*/min. For a typical sample of 1 *ℓ* the exposure rate was also two times per minute.
- The flow rate for the PTH unit was 35 *ℓ*/min. For a typical sample of 10 *ℓ* the exposure rate was 3.5 times per minute.

Cleaning of the PVC test loops was done with 10% nitric acid but the devices were rinsed with dilute acetic acid to prevent acid damage to metal surfaces.

The exposure rate is a function of flow rate and total volume of the test solution and was determined by the capacity of the pumps and practical test volumes. It was not necessary to keep exposure rates the same for all three test devices.

Instrumentation

For elemental analysis an ARL 35000 inductively-coupled plasma optical emission spectrometer(ICP-OES), VGA plasma Quad 2 + ICP mass spectrometer(ICP-MS) and GBC 909 atomic absorption spectrometer (AAS) were used. The limit of quantitative

TABLE 1
CHEMICAL ANALYSIS OF TAP WATER (ALL CONCENTRATIONS IN mg/ℓ EXCEPT WHERE INDICATED OTHERWISE)

Parameter	Quantity	Parameter	Quantity	Parameter	Quantity
Conductivity (μS/cm)	125	Boron	<0.1	Selenium (μg/ℓ)	<0.1
Turbidity (NTU)	0.7	Cobalt	<0.1	Active silica	2.6
pH	7.96	Copper	<0.1	Total silica	4.0
Alkalinity ($CaCO_3$)	76	Iron	<0.05	Ammonia as N	0.12
Hardness ($CaCO_3$)	78	Manganese	<0.03	Orthophosphate as P	0.03
Calcium	19	Lead	<0.03	Nitrate as N	0.23
Magnesium	7.6	Zinc*	<0.1	Nitrite as N	0.11
Sodium	17	Nickel	<0.1	Chloride	14
Potassium	4	Aluminium	0.15	Fluoride	0.28
Cadmium (μg/ℓ)	<30	Mercury (μg/ℓ)	<0.1	Sulphate	16
Chromium	<0.05	Arsenic (μg/ℓ)	<0.1	Phenol (μg/ℓ)	1.1

* Zinc concentrations were found to vary from day to day between 40 and 60 μg/ℓ

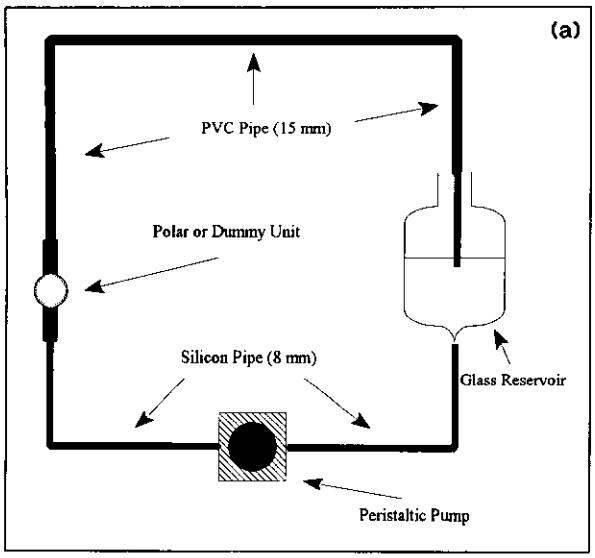

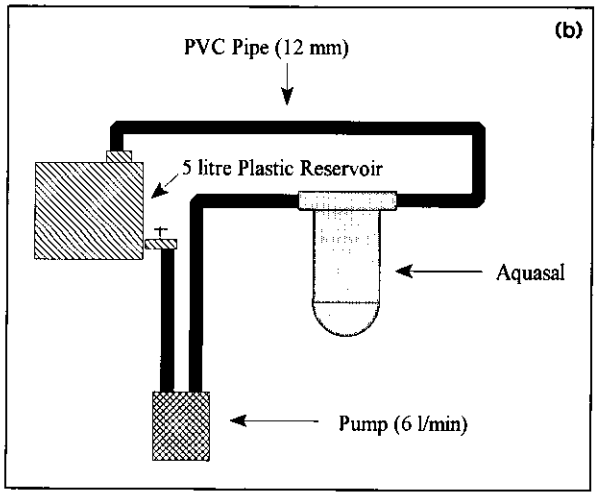

Figure 3
(a) Test loop for Polar antiscaling device
(b) Test loop for Aquasal and PTH antiscaling devices

determination for zinc on the GBC 909 AAS was sufficiently low to determine background levels of zinc in the experimental systems used in this investigation. For other metals, the ICP-MS was used to determine background concentrations. Calcium in test solutions was routinely monitored with ICP-OES.

pH measurements were made with an Orion 940 pH meter.

Crystal morphologies of precipitated $CaCO_3$ scale were determined with an ISI-SS60 scanning electron microscope (SEM) and the corresponding crystal structure by X-ray diffraction (XRD) using a Phillips PW1729 diffractometer.

Zeta potentials and particle sizing were determined by photon correlation spectroscopy (PCS) using a Malvern Zetamaster.

Zinc speciation studies were done by voltammetry using a Metrohm 626 Polarecord and Metrohm 662 VA stand.

Solutions

A sufficiently stable supersaturated $CaCO_3$ solution with suitable scale-forming potential was prepared by bubbling CO_2(g) using a glass frit as dispersing nozzle, through a suspension of 3.8 g of $CaCO_3$ (Merck analar) in 5 ℓ of water for 1 h. The suspension was suction-filtered rapidly through 0.45 μ Millipore cellulose acetate membrane filters to remove undissolved $CaCO_3$ and the calcium concentration determined by ICP-OES. Deionised water with an electrical resistance of 18MΩ prepared with a Millipore polishing unit and tap water with a typical composition summarised in Table 1 were used. The required final concentration for $Ca(HCO_3)_2$ solutions was obtained by dilution of the ca 300 mg/ℓ Ca stock solution with deionised water.

Methods

Cleaning of glassware

All glassware was treated with 10% nitric acid for 12 h, thoroughly rinsed with deionised water and then steam-cleaned to remove all insoluble particles that might adhere to inner glass surfaces.

Metal emissions from PWT devices

Metal emissions from the PWT devices were determined by pumping 1 ℓ of deionised water or 0.001 M KCl through the test loop for 1 h with the particular device inserted. Metal concentrations were then determined by ICP-MS. The conductivity of the 0.001 M KCl solution was 126 $\mu S \cdot cm^{-1}$ which simulated the typical conductivity of local tap water.

Crystallisation kinetics

Kinetics of $CaCO_3$ crystallisation from supersaturated $CaCO_3$ solutions were studied by using a batch method in which a test and control could be run simultaneously in triplicate. $CaCO_3$ solutions were always supersaturated. The concentration was, however, chosen in such a way that the solution was metastable with regard to precipitation. This means that precipitation could take place thermodynamically but kinetically the nucleation rate was too slow. Precipitation thus only started after prolonged heating at 37°C. Extreme care was taken to ensure that all experimental conditions were exactly the same for test and control run. These included the parameters: temperature, concentration, age of solution, condition of glassware, and pH.

$CaCO_3$ solutions, made up with deionised water or tap water, typically 150 mg/ℓ Ca, were circulated in the test loop with or without device for 10 min. Aliquots from the same stock solution were used for test and control runs. 200-mℓ samples in triplicate of the treated solutions were transferred to 250 mℓ glass beakers, covered with Parafilm and placed on a multi-point magnetic stirrer assembly (the rate of stirring was exactly the same at all stirring positions) in a waterbath at 37°C after a predetermined waiting time, typically 15 min. The pH of six solutions, three tests and three controls, was followed simultaneously as a function of time for up to 6 h. The same pH probe was used to monitor all six solutions to ensure comparability of the measurements.

Crystal morphology and crystallography

Crystals were collected when the crystallisation process was completed, vacuum-dried and small amounts mounted for SEM analysis or prepared for XRD. Calcite, aragonite and vaterite crystal forms were easily identified by scanning electron microscopy by recognising the calcite rhombohedrons, aragonite needles and vaterite discs. Crystal morphology is an important parameter in determining the properties of scale. Calcite is usually associated with a hard scale whereas aragonite and vaterite could give rise to a softer type of scale that is easily removed. No consensus has, however, been reached on this issue. It was also possible to estimate the percentage composition in samples where mixtures of crystal morphologies occurred. Crystal structures were then confirmed by XRD.

Results and discussion

Precipitation chemistry of $CaCO_3$

A brief review of the basic precipitation chemistry of $CaCO_3$ would facilitate the interpretation of results obtained in the crystallisation kinetic experiments and is given below. A fundamental aspect of scale formation involving $CaCO_3$ is the relationship between CO_2(aq) concentration in the solution and the solubility of $CaCO_3$ and the effect of temperature on this solubility. The solubilty of $CaCO_3$ varies inversely with temperature. On heating CO_2 escapes, favouring the bicarbonate decomposition reaction followed by $CaCO_3$ precipitation:

$$2HCO_3^- = CO_2(aq) + CO_3^{2-} + H_2O$$
$$Ca^{2+} + CO_3^{2-} = CaCO_3(s)$$
$$\overline{Ca^{2+} + 2HCO_3^- = CaCO_3(s) + CO_2(aq) + H_2O}$$

At temperatures < 50 °C calcite is the preferred crystal structure and at temperatures > 60°C aragonite predominates. In the region between 50 and 60°C both forms can occur. It must also be kept in mind that aragonite ($K_{sp} = 4.6\times10^{-9}$) is slightly more soluble than calcite ($K_{sp} = 3.3\times10^{-9}$). A third form, vaterite which is unstable and transforms into calcite especially at high temperatures, also occurs occasionally. It is very rare and for all practical purposes does not exist in nature.

The metastable region for $CaCO_3$ is exceptionally large. This region is characterised by the non-precipitation of $CaCO_3$ despite the fact that the solution is supersaturated. The phenomenon is caused by the fact that nucleation is limited by the relatively high solubility of microscopically small crystals initially formed during nucleation. The width of the metastable region is given thermodynamically by the free energy of formation of a nucleus in homogeneous nucleation. This energy can be lowered by metal surfaces or by the presence of colloidal particles that might act as seed crystals whereby the width of the metastable region is decreased. This is called heterogeneous nucleation and is the dominant mechanism during scale formation. This phenomenon made it possible to prepare supersaturated metastable solutions which could be used in time-dependence experiments without danger of premature precipitation occurring.

Crystallisation kinetics

The crystallisation reaction of $CaCO_3$ can conveniently be studied by following the pH of the precipitating solution as a function of time. The data from these experiments can then be presented graphically as precipitation curves, which are plots of pH vs. time. Precipitation curves obtained for the three antiscaling devices are shown in Fig. 4 (top) for the (a) Polar, (b) PTH, and (c) Aquasal devices. The equivalent curves for the controls are included in each case.

The curves can be interpreted by referring to the above-mentioned chemical equilibria. The initial rise in pH with time is caused by the removal of CO_2 from the solution as the temperature is increased from ambient to 37°C. Typically the experimental temperature of 37 °C was obtained in the test solutions within 5 min after introducing the test solutions to the waterbath. The sharp downward adjustment of the pH marks the onset of the precipitation of solid $CaCO_3$. It was also possible to confirm this by the visible appearance of a slight milkiness in the solutions. The time interval required for the precipitation to start, the induction period, could be determined in this way.

Investigation of the crystal morphology of the precipitates by scanning electron microscopy provided another experimental parameter to obtain information with regard to possible effects on the pecipitation process.

The measurable effects caused by the three units on the crystallisation process of $CaCO_3$ were compared to those observed for the controls and are summarised in Table 2. These effects were:

- increase in induction time i.e. the time needed for the precipitation reaction to begin
- formation of $CaCO_3$ in the aragonite form rather than calcite.

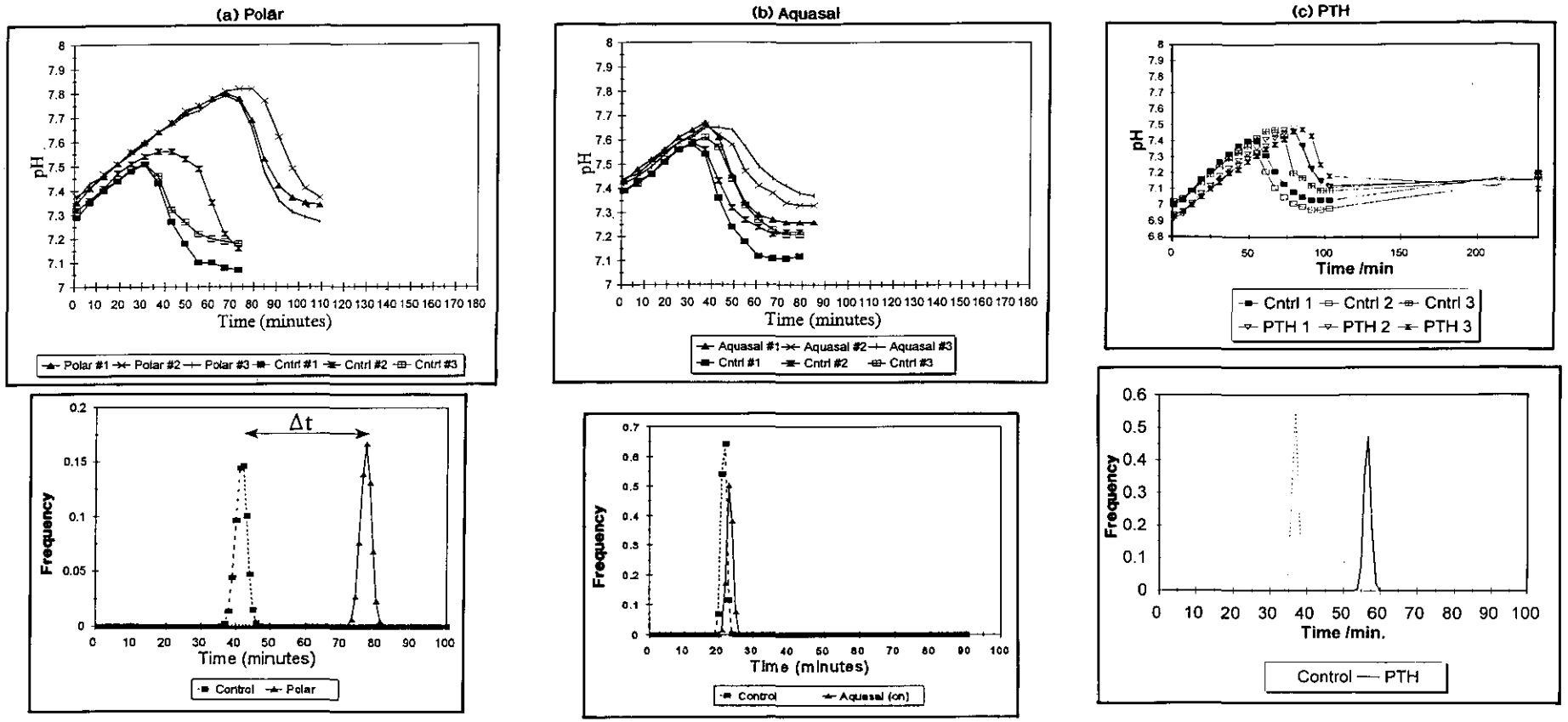

Figure 4

***Top**:Typical precipitation curves for $CaCO_3$ from $Ca(HCO_3)_2$ solutions that were exposed to an antiscaling device and its control (a) Polar (b) Aquasal (c) PTH*

***Bottom:** Gaussian distributions of induction times for $CaCO_3$ precipitation for treated and non-treated $Ca(HCO_3)_2$ solutions showing the average delay time, Δt. (a) Polar (b) Aquasal (c) PTH*

TABLE 2
OBSERVED DELAY TIMES, Δt, AND CRYSTAL FORM OF PRECIPITATES FOR DIFFERENT PWT DEVICES

Device	Δt min	Crystal form	µg/ℓ of Zn released/ 10 min
Polar	35±4	80-100% aragonite	100
Polar coated	0	100% calcite	0
Aquasal	6±2	50-80% aragonite	14
Aquasal coated	0	100% calcite	0
PTH	20±1	50-80% aragonite	20
PTH coated	0	100% calcite	0
Control	0	100% calcite	0
Zn added to control	33±4	100% aragonite	100

TABLE 3
AMOUNT OF METAL RELEASED (µg/ℓ·h) INTO A 0.001 M KCl SOLUTION AT CONSTANT FLOW RATES AS REQUIRED BY EACH DEVICE (SEE EXPERIMENTAL)

Element	Polar	Polar blank	Aquasal	Aquasal blank	PTH	PTH blank
Al	10	<10	<10	<10	<10	<0
Ba	<10	<10	<10	<10	<10	<10
Co	54	<5	<5	<5	<5	<5
Cr	<5	<5	<5	<5	<5	<5
Cu	<5	<5	<5	<5	24	<5
Fe	<100	<100	<100	<100	<100	<100
Nd	<10	<10	<10	<10	<10	<10
Ni	10	<10	<10	<10	78	<10
Zn	589	8	124	15	118	8

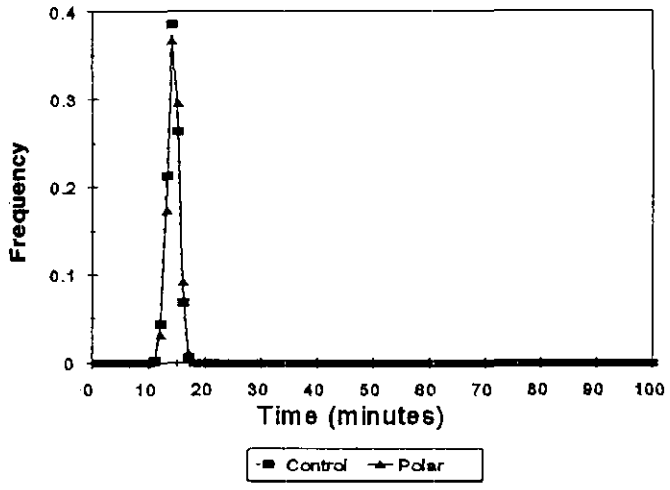

Figure 5
Gaussian distributions of induction times for coated Polar unit showing zero delay time between control and treated solution

The effective delay time, Δt, was determined from the difference between the average induction time observed for the device and that of the control. The standard deviation for each set was used to calculate a Gaussian distribution for the measured induction times. Graphical representations of these distributions, which illustrate the statistical significance of the delay time are shown in Fig. 4 (bottom) for (a) Polar, (b) Aquasal and (c) PTH devices.

In subsequent experiments all internal surfaces that came into contact with the test solution were coated with a silicone based liquid polymer (Dow Corning R43117) in order to determine whether contact of the solution with the internal surfaces was of any consequence. Results showed that by eliminating direct contact with internal surfaces the delay times for all devices were essentially reduced to zero. That means no observable difference in induction times was evident when compared with the controls. A typical result is given in Fig. 5. This result obviously pointed to an effect caused by some surface reaction or the release of species from the surface which might increase the nucleation time of $CaCO_3$ solutions.

The amount of impurities introduced into the solution was determined for each device by circulating a known volume of 0.001 M KCl solution in deionised water at a constant flow rate for one hour. The metal concentrations were determined by ICP-MS and the results are summarised in Table 3. The POLAR and AQUASAL units released substantial quantities of zinc while for the PTH unit other metals like copper and nickel were found. In subsequent experiments the release rate of metals was found to be linear with time.

It was found that the effectiveness of the devices tended to

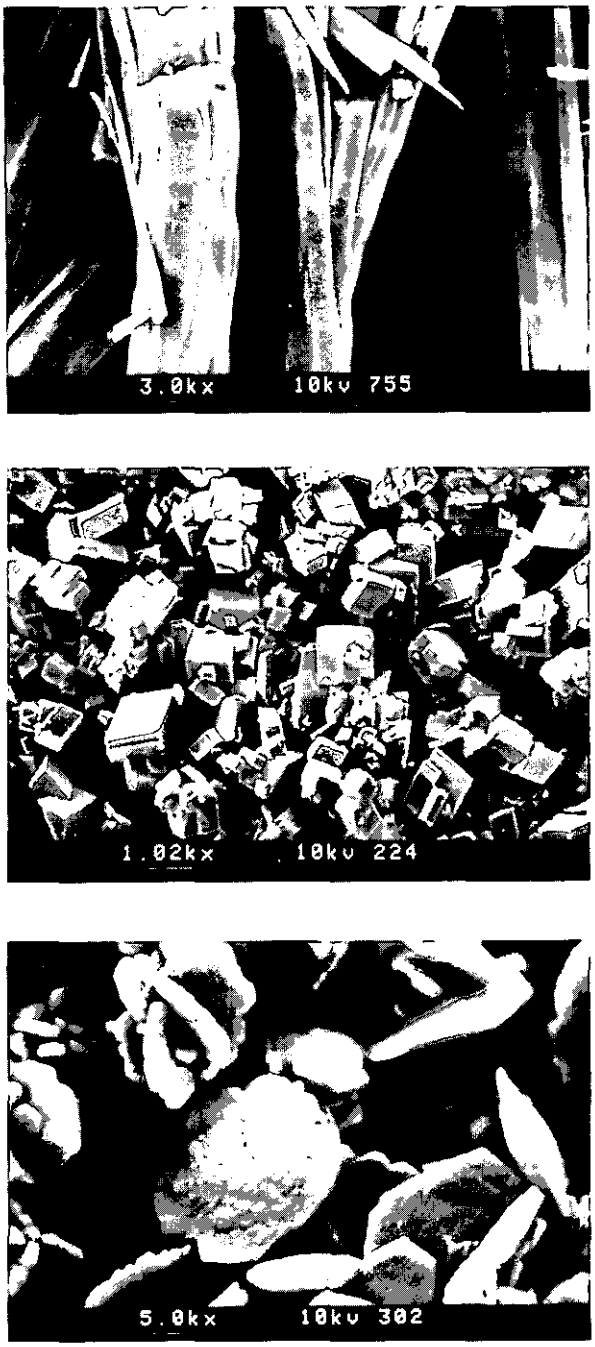

Figure 6
Scanning electron micrographs showing typical (a) calcite (b) aragonite (c) vaterite crystals obtained from the precipitation of treated and untreated $Ca(HCO_3)_2$ solutions

deteriorate with time during frequent use. This was caused by scale build-up on the internal surfaces effectively reducing the amount of metal ions released into the feed stream. After cleaning the surfaces with dilute acetic acid the emission values recovered and the same delay times as before were observed. In the case of the Polar, Zn emissions from the magnet and the Zn sleeve in the strainer were of similar magnitude. The amount of zinc released per cycle ranged from 5 µg/ℓ for the Polar, 0.5 µg/ℓ for the PTH and 0.4 µg/ℓ for the Aquasal. The rate of metal release is strongly dependent on the conductivity of the circulating solution. The rate in deionised water was approximately 10 times lower than for 0.001M KCl.

Crystal morphology

Scanning electron microscopy of the precipitated crystals revealed a consistent pattern for all three devices and is summarised in Table 2. Treated solutions consistently produced $CaCO_3$ in the aragonite form whereas the controls gave calcite. Occasionally treated and untreated solutions gave rise to $CaCO_3$ precipitating in the vaterite form. This seemed to appear at random and no correlation between its formation and experimental conditions could be established. Typical crystal morphologies are shown in Fig. 6.

When the internal surfaces were coated, the crystal morphology reverted to calcite. It should be pointed out that calcite would be the preferred crystal form under the experimental conditions used, because $CaCO_3$ crystallises in the calcite form at temperatures below 40°C. It is known that trace impurities present in a solution during precipitation can alter the crystallographic form. It is also known that trace impurities inhibit the crystal growth rate of $CaCO_3$ (Meyer, 1984). Both these facts point to the role of metal impurities especially zinc, in explaining the observed effects of three different physical water treatment devices.

The Zn hypothesis

In order to prove this hypothesis a number of experiments were conducted in which small amounts of Zn^{2+} ions were added to supersaturated $CaCO_3$ solutions containing 150 µg/ℓ Ca. The crystallisation reaction was then followed as before at 37°C and the precipitation curves compared.

The concentration of Zn generated in a $CaCO_3$ solution, 150 µg/ℓ with respect to Ca, and which was exposed to the Polar device for 10 min, was ca. 100 µg/ℓ. The average delay time measured for this solution was 35±3 min. By adding 100 µg/ℓ of Zn as freshly prepared $ZnSO_4$ to a $CaCO_3$ solution containing 150 µg/ℓ Ca, an average delay time of 33±4 min was obtained. Actual precipitation curves for $Ca(HCO_3)_2$ solutions containing 50 µg/ℓ Zn are shown in Fig. 7. Further support came from the fact that the crystal morphology was aragonite rather than calcite. These results were repeated consistently for different Zn concentrations and different Ca concentrations. A comprehensive systematic study by the same authors of the effect of Zn species on scaling reactions is underway and will be reported separately.

Memory effect

It is claimed by manufacturers that the effects of PWT devices are still noticeable for periods of up to 72 h after treatment. In a series of experiments, 50 µg/ℓ of freshly prepared $ZnSO_4$ solution was added to four supersaturated $CaCO_3$ solutions . These solutions were then equilibrated for different waiting periods ranging from 1 min to 24 h after which precipitation reactions were induced as before. Delay times gradually decreased with time but were still measureable after 24 h.

Polarographic results obtained by following the height of the zinc polarographic peak after introducing 50 µg/ℓ of freshly prepared $ZnSO_4$ into an 0.001 M $NaHCO_3$ solution revealed a slow decrease in peak height over time. This indicated the transformation of free zinc into polarographically inactive species. By implication these species could also be less effective in

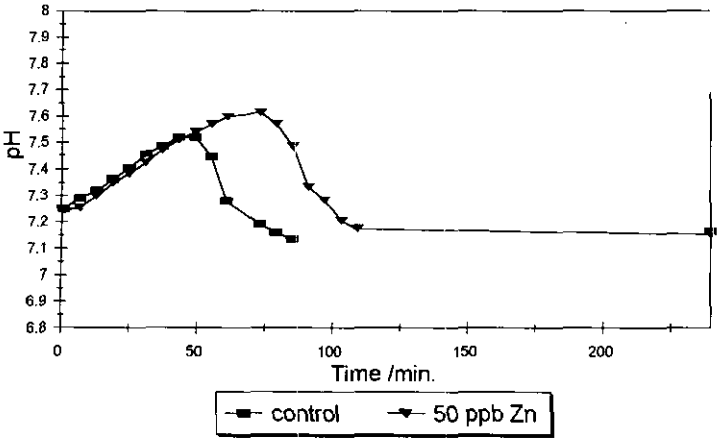

Figure 7
Typical precipitation curves for $CaCO_3$ from $Ca(HCO_3)_2$ solutions containing 50 µg/ℓ Zn vs. the control containing no Zn

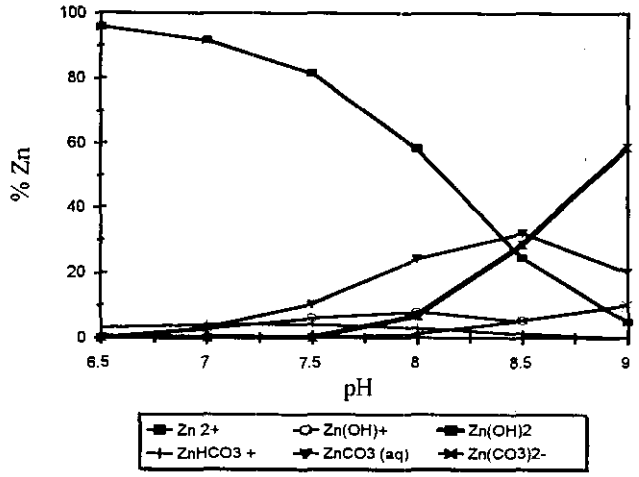

Figure 8
Species distribution diagram for the $ZnSO_4/NaHCO_3$ system, $[Zn]_{tot}$ = 50 µg/ℓ and $[HCO_3]_{tot}$ = 0.001 M

influencing the $CaCO_3$ crystallisation reaction. Adsorption of zinc species could also have been responsible for the observed reduction in peak heights. However, a similar experiment using an 0.001 M KCl solution to which 50 µg/ℓ zinc was added produced no change in zinc peak height over a 24-h period. The speciation in such a solution is, however, different with chloro complexes of zinc predominating.

Speciation calculations for the zinc/bicarbonate system using Minteqa2 (Allison et al., 1991) produced the distribution diagram in the pH range 6.5 to 9 shown in Fig. 8.

At pH above 7.5, which was typical for the solutions studied, the zinc carbonate complex species, $ZnCO_3(aq)$ and $Zn(CO_3)_2(aq)$ were predominant. These complexes are relatively stable, effectively preventing the hydrolysis of Zn^{2+} to $Zn(OH)_2(s)$ which would normally occur at this pH.

One could speculate on the relative ineffectiveness of a neutral species like $ZnCO_3(aq)$ to block growth sites on $CaCO_3$ crystals if one assumes a surface adsorption mechanism as part of the scale forming process. It is however beyond the scope of this investigation to present a proper mechanistic explanation of the observed phenomena. Further work is in progress to study possible mechanisms.

Conclusion

We have shown that the emission of zinc from three different types of physical water treatment devices can affect the rate of calcium crystallisation and also can cause changes to the crystal morphology of the precipitates. It is suggested that these effects may have the potential to alter the scaling characteristics of water treated with these devices. We could find no measureable effects that could be related to any of the physical fields, be they magnetic or electric. We have also shown that the effect is dependent on the introduction of "fresh" Zn^{2+} ions into the water prior to the antiscaling application. The active form of zinc was shown to have an operational lifetime of at least 24 h.

Acknowledgement

We thank the Water Research Commission of South Africa for financial support.

References

ALLISON JD, BROWN DS and NOVO-GRADAC KJ (1991) MINTEQA2/PRODEFA2, a geochemical assessment model for environmental systems. *EPA/600/3-91/021.*

BAKER JS and JUDD JJ (1996) Magnetic amelioration of scale formation. *Water Res.* **30**(2) 247-260.

BUSCH KW, BUSCH MA, PARKER DH, DARLING RE and McCATE E JL (1986) Studies of a water treatment device that uses magnetic fields. *Corrosion* **42**(4) 211-221.

CAPLAN C and STEGMAYER F (1987) Field study: Electromagnetic device used to treat a watertube boiler. *Int. Water Conf.* **28** 267-274.

ELIASSEN R and UHLIG H (1952) So-called electrical and catalytic treatment of water for boilers. *Jawwa* **44** 576-582.

ELLINGSEN FT and FIEDSEND O (1982) A revue of scale formation and scale prevention, with emphasis on magnetic water treatment. SSIWSA Congress, 8-12.

KOCHMARSKII VZ, KUL'SKII LA and KRIVTSOV VV (1982) After effects of magnetic antiscale treatment. *Khimiya i Tekhnologiya* **4** 217-222.

MEYER HJ (1984) The influence of impurities and the growth rate of calcite. *J. Cryst. Growth* **66** 639-646.

PANDOLFO L, COLACER and PAIARO G (1987) Magnetic field and tap water. *Chimica e l'Industria* **69** 88-89.

VAN DER HOVEN TH, JJ, BRINK H and VAN EEKEREN M WM (1991) Ervaringen met EAK-apparaten zoals befend bij de waterleidingsbedrijven in Nederland. *Water* **24** 734.

VERMEIREN T (1953) Magnetic treatment of liquids for scale and corrosion prevention. *Corrosion Technol.* (July) 215-219.